Conf. 790125--6

MASTER

LA-UR-79-23

TITLE: DIFFERENTIAL NEUTRON CROSS SECTION FOR FREE INTERSTITIAL PRODUCTION IN COPPER

AUTHOR(S): Joyce A. Goldstone, Don M. Parkin, and Hoyle M. Simpson

SUBMITTED TO: American Nuclear Society Meeting, Fusion Reactor Materials Conference, Miami Beach, FL, January 29-31, 1979

los alamos scientific laboratory
of the University of California
LOS ALAMOS, NEW MEXICO 87545

An Affirmative Action/Equal Opportunity Employer

Form No. 836
St. No. 2629
1/75

UNITED STATES
ENERGY RESEARCH AND
DEVELOPMENT ADMINISTRATION
CONTRACT W-7405-ENG. 36

DIFFERENTIAL NEUTRON CROSS SECTION FOR FREE INTERSTITIAL PRODUCTION IN COPPER*

J. A. GOLDSTONE, D. M. PARKIN, and H. M. SIMPSON†

Los Alamos Scientific Laboratory, Los Alamos, NM 87544

Free interstitials produced by monoenergetic neutrons were monitored by changes in Young's modulus of a vibrating foil specimen. These changes can be related to the number of pinners on dislocations which depends on the number of defects produced. The pinning rate is compared with displacement cross section calculations and agrees with the Norgett-Robinson-Torrens (NRT) model. Electron irradiations on the same sample yield estimates of the free interstitial production cross section to be ∿ 1% of the NRT cross section.

1. INTRODUCTION

Herein we describe the first experiment in which the production rate of free interstitials in copper was studied as a function of monoenergetic neutron energy from 2 to 24 MeV. The pinning rate of dislocations by interstitials[1] was monitored during irradiation by changes in Young's modulus of a vibrating foil specimen. This technique offers several advantages over previous damage studies: (1) the sensitivity of Young's modulus to low defect concentrations (1 part in 10^{13}) ensures that complications due to defect interactions do not arise and that good response is obtained at low ($10^{11} m^{-2} s^{-1}$) neutron flux levels; (2) the use of monoenergetic neutron sources aids in the evaluation of the neutron flux and comparison to theoretical displacement cross sections; (3) continuous monitoring of changes during irradiation is possible; and (4) the same sample can be irradiated with both neutrons and electrons. Furthermore, we have designed this experiment so that dislocation dynamics and diffusion kinetics do not play a critical role in conclusions drawn from the data.

Schematically, in Fig. 1, the fate of interstitials produced during irradiation is illustrated. We ignore the migration of the vacancies since their motion is slow compared to the interstitial and the free interstitial is the defect responsible for dislocation pinning in this experiment. During electron irradiation, isolated interstitial-vacancy (I-V) pairs are produced. Either the interstitial recombines with its vacancy or escapes to freely migrate in the lattice. During migration various fates await; eg. trapping, annihilation, or dislocation pinning. In the cascade structure produced by neutron irradiation, multiple I-V pairs are created; however some interstitials escape to freely migrate and suffer the same fate as electron-produced interstitials. Since in our experiment we observe those interstitials which reach dislocations, no distinction between neutron or electron-produced interstitials can be made. Our experimental data[2] supports the above argument: the flux dependence and temperature dependence of the initial pinning rate is identical for 0.5 MeV electron and 14.1 MeV neutron irradiations.

Dislocation damping measurements show that the modulus decreases monotonically during irradiation indicating that dislocations are

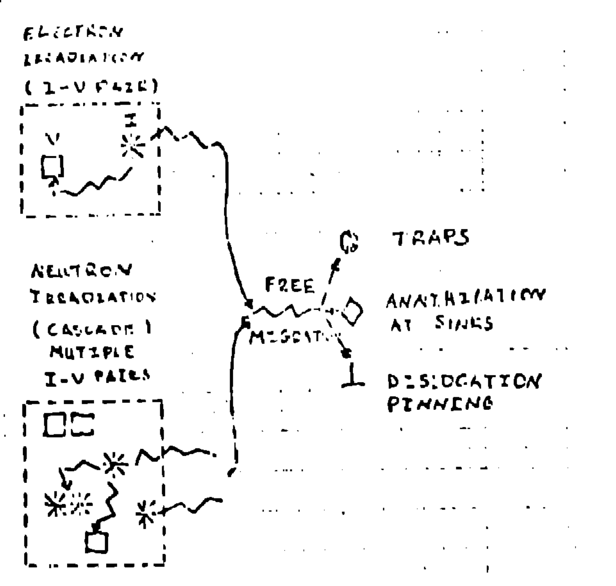

Fig. 1. Freely migrating interstitials produced by either electron or neutron irradiation behave identically in the lattice.

*Work supported by the Department of Energy and Associated Western Universities.

†Permanent Address: Physics Department, Wright State University, Dayton, OH 45431

restricted in their motion by the defects produced. In this experiment, we develop a correlation between the free interstitial production rate and the rate of change of Young's modulus during electron irradiation. This functional correlation does not require a model to relate pinning rate and defect production rate since the same sample is used in all experiments and the correlation is derived only in a relative sense. One can take the pinning rate as a measure of defect production rate as long as pinning rates are determined at the same value of pinning point concentration (in our case: zero) and same value of time derivative of pinning point concentration (our data is scaled from the flux dependence curves)[3]. The parameter we use to represent the modulus change is given by the Simpson-Sosin model[4]:

$$\frac{(\Delta E/E)_o}{(\Delta E/E)} - 1 \equiv N_{dy} = \frac{\tau_o^2 - \tau^2}{\tau^2 - \tau_e^2}$$

where $\Delta E/E$ is the modulus defect, τ is the inverse resonant frequency and the subscripts o and e refer to the initial and elastic (fully pinned) values.

2. EXPERIMENTAL

All irradiation experiments were performed on the same high purity (99.999%) copper sample. The sample was machined from material supplied by ASARCO into the form of a cantilevered beam, 0.076 mm thick, with a flexural resonant frequency of 770 Hz. The sample temperature was held at 330 K during irradiation and the sample was annealed in situ at 773 K for 10 minutes between irradiations to eliminate defects created by the previous irradiation. This procedure reproduced the initial value of Young's modulus prior to irradiation, thus experiments were performed on the one and same sample[3]. Changes in Young's modulus at constant strain amplitude ($< 10^{-6}$) were monitored continuously through changes in the resonant frequency which was tracked and recorded by the automatic data logging system[4].

Electron irradiations were performed at Wright State University with 0.5 MeV electrons over a flux range of 10^{13} to $10^{15} m^{-2} s^{-1}$ resulting in free Frenkel pair production rates of 10^{12} to $10^{15} m^{-3} s^{-1}$. The fully pinned state was obtained by raising the beam energy to 1 MeV and the flux to $3 \times 10^{16} m^{-2} s$ and irradiating to saturation. Neutron irradiations at 14 MeV were done at the Cockcroft-Walton accelerator at LASL where the flux was varied from 10^{11} to $2 \times 10^{12} m^{-2} s$. An associated alpha particle counter was used for flux measurements. Energy dependent neutron experiments were done at the tandem Van de Graaff at LASL where neutron energies from 2 to 24 MeV were available. Dosimetry foils gave the integrated flux, while a scintillation counter allowed continuous monitoring of the flux. Through knowledge of the source geometry and reaction kinematics, flux values at the dosimeter position were converted to flux values at the sample to an accuracy of 10%. Table I gives the reaction, incoming particle energy, the neutron energy at the sample, the dosimeter, and the flux at the sample.

3. DISCUSSION

Figure 2 shows a representative plot of N_{dy} versus time for an irradiation with 6 MeV neutrons. The pinning rate due to neutron created defects is the difference in slope of straight line fits to the data before and after the irradiation was begun. Dividing by the flux and normalizing to the 14 MeV datum point, the relative pinning versus neutron energy is obtained as shown in Fig. 3.

The measured neutron energy dependent pinning rate can be compared with displacement cross section calculations. The displacement cross section is given by [6]:

$$\sigma_D(E) = \int_{E_d}^{T_{max}} \sigma(E)\ K(E,T)\ g(T) dt$$

where $\sigma(E)K(E,T)$ is the total recoil probability cross section. The function $g(T)$ correlates the kinetic energy of a recoiling atom with the number of Frenkel pairs produced. Three forms of $g(T)$ are respectively the NRT, [7,8,9] RT-b[10,11] and RT-3[11] models:

$$\begin{aligned} g(T) &= 0.8 T_{dam}/2E_d \\ &= .0166[1 - 0.04 \ln(T_{dam} \times 10^{-3})] T_{dam} \\ &= T_{dam}/[58 + (1.25 \times 10^{-3}) T_{dam}] \end{aligned}$$

where $T_{dam}(eV) = TL(T)$ where $L(T)$ is the Lindhard electronic energy loss factor[12], and E_d is the energy required to displace an atom. Both the RT-b and RT-3 models equally well fit the RT computer simulation data, but have quite different projections to high energy. On Fig. 3, the relative values of these three curves are plotted as "best fits" to the data points, so as to compare the slope of the models with the data. It can be seen that agreement with NRT or RT-b formalism is very good, but the RT-3 dependence does not describe the energy dependence at all.

Table I
Experimental Neutron Energies and Fluxes

Reaction	Incoming Particle Energy (MeV)	Neutron Energy (MeV)	Dosimetry	Neutron Flux ($m^{-2} s^{-1}$)
$H(t,n)^3He$	$4.4 \pm .2$	$1.9 \pm .1$	In foil	$1.2 \pm .1 \times 10^{12}$
$H(t,n)^3He$	$6.9 \pm .1$	$3.9 \pm .1$	In foil	$1.4 \pm .1 \times 10^{12}$
$H(t,n)^3He$	$9.6 \pm .1$	$5.9 \pm .1$	In foil	$1.4 \pm .1 \times 10^{12}$
$T(d,n)^4He$	$0.30 \pm .03$	$14.1 \pm .1$	α-monitor	$1.0 \pm .7 \times 10^{12}$
$D(t,n)^4He$	$6.0 \pm .2$	$23.4 \pm .1$	Al foil	$2.1 \pm .2 \times 10^{11}$

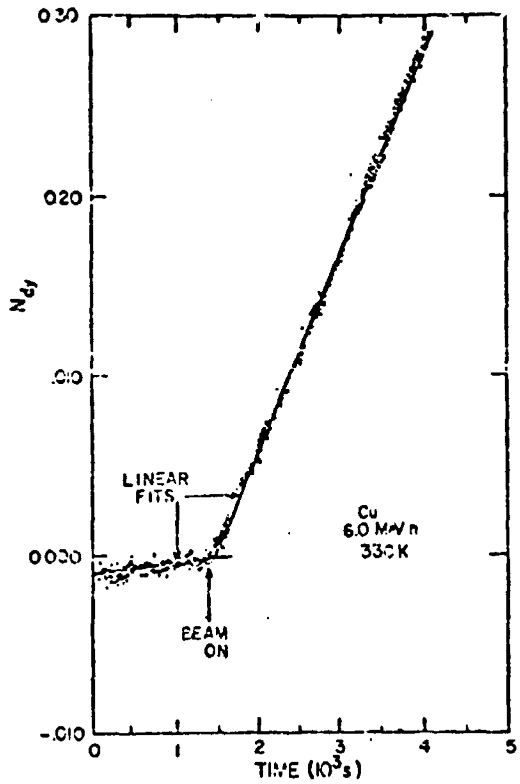

Fig. 2. The number of pinning points added to the dislocation lines versus time. The sample temperature is 330 K and the neutron flux is $1.4 \times 10^{17} m^{-2} s^{-1}$ at 6 MeV.

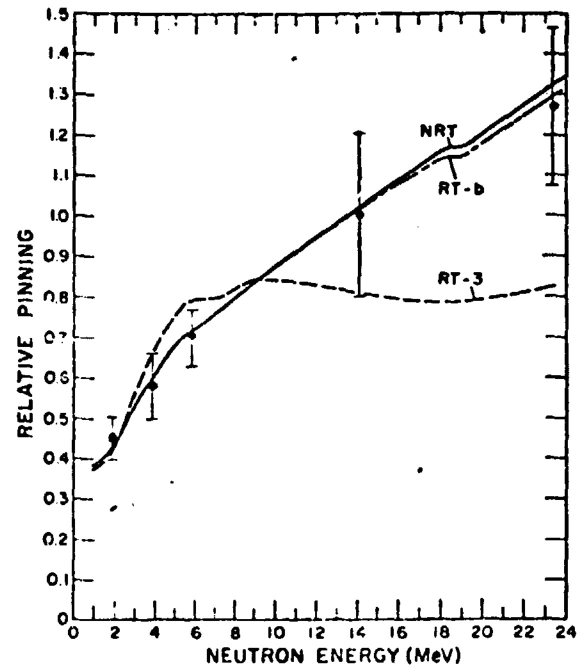

Fig. 3. The relative pinning versus neutron energy from the modulus data. The curves are three forms of the energy dependence of neutron damage.

By comparison with electron irradiations, estimates of the free interstitial production cross section $(f\sigma_D)^n$ can be made:

$$dN_{dy}/dt \propto \rho\phi(f\sigma_D)$$

where ρ = number density, ϕ = flux, and f = fraction of interstitials remaining free at high temperatures (0.25 for the electron case as measured by electrical resistivity techniques[13]). For equal initial pinning rates:

$$(f\sigma_D)^n = (f\sigma_D)^{e-}\phi^{e-}/\phi^n.$$

Evaluation of $(\sigma_D)^{e-}$ is difficult due to conflicting results when comparing low temperature resistivity measurements[14], high temperature dislocation pinning measurements[3] and theoretical displacement cross sections[15]. We estimate $(\sigma_D)^{e-} = 5.9 \times 10^{-28} m^2$ is within a factor of 2 of the true cross section. Thus order of magnitude estimates of $(f\sigma_D)^n$ and f^n can be established. Table II gives the calculated NRT cross sections, $(\sigma_D)^n$, and the experimental free interstitial production cross section, $(f\sigma_D)^n$, for each neutron energy. It can be seen that the percentage of free interstitials is a small fraction of the predicted numbers of Frenkel pairs. The given errors in $(f\sigma_D)^n$ and f^n are based on the data analysis and do not reflect errors in $(f\sigma_D)^{e-}$.

The validity of the comparison of the experimental free interstitial production cross section to the calculated total defect production cross section is based on the nature of the displacement cascades at high recoil energies. Robinson[16], in a qualitative discussion, suggested that in the regime where electronic energy losses cannot be ignored, the fraction of total defects surviving in the cascade is nearly constant with increasing recoil energy and the defect density is independent of recoil energy. Thus, the fraction of free interstitials is nearly constant for these recoil energies. From the computer simulations

Table II
Free Interstitial Production Cross Sections

Neutron Energy (MeV)	$f\sigma_D$(exp) ($10^{-28} m^2$)	σ_D(NRT) ($10^{-28} m^2$)	f^n
1.9	13 ± 4	1275	$.010\pm.003$
3.9	10 ± 6	2150	$.008\pm.003$
5.9	20 ± 7	2790	$.007\pm.003$
14.1	32 ± 3	4400	$.007\pm.001$
23.4	38 ± 13	6050	$.006\pm.002$

of Doran et al.[17] this leveling off process in cascade structure occurs around 5 KeV. Experimentally, Merkle[18] observed that the size distribution of defects in ion-irradiated copper remained unchanged with increasing irradiation energy. Defect-production efficiency measurements by Averback et al.[19] and Kirk and Greenwood[20] in copper have shown constant efficiency relative to the NRT model for ion and neutron irradiations. Roberto et al.[21] have concluded that in copper the primary damage state remains essentially unaltered as the mean neutron energy increases from 2 to 15 MeV. Therefore large changes in f^n are not expected nor observed (see Table II). The decrease observed in f^n, although consistent with an interpretation of increasing defect density as recoil energy increases, is not considered significant since it is within the experimental errors.

These damage rate experiments provide the first pointwise damage cross sections for the production of free interstitials measured at elevated temperatures. Damage cross sections are an important tool in correlating radiation damage results obtained from a variety of sources. Experimental measurements of damage cross sections above 14 MeV are of particular importance to the utilization of Be(d,n) and Li(d,n) neutron sources.

The authors are grateful for the help received from B. Dayhurst and J. Gilmore of LASL in counting dosimetry foils and calculating neutron fluxes and R. K. Smith for his assistance in doing experiments at the LASL Van de Graaff.

References

[1] H. M. Simpson and S. J. Keikhoff, Radiat. Eff. 27 (1976) 191,197.

[2] J. A. Goldstone, Ph.D Thesis, SUNY at Stony Brook (1978).

[3] G. Roth, H. Wollenberger, Ch. Zeckav, and K. Lücke, Radiat. Eff. 26 (1975) 141.

[4] H. M. Simpson, A. Sosin, and D. F. Johnson, Phys. Rev. B 5 (1972) 1393.

[5] H. M. Simpson and A. Sosin, Rev. Sci. Instrum. 49 (1977) 1392.

[6] D. M. Parkin and A. N. Goland, Radiat. Eff. 28 (1976) 31.

[7] M. J. Norgett, M. T. Robinson, and I. M. Torrens, Nucl. Eng. Des. 33 (1975) 50.

[8] G. H. Kinchin and R. S. Pease, Rep. Prog. Phys. 18 (1955) No. 1.

[9] M. T. Robinson, Philos. Mag. 12 (1965) 741.

[10] J. R. Beeler, Phys. Rev. 150 (1966) 470.

[11] M. T. Robinson and I. M. Torrens, Phys. Rev. B 9 (1974) 5008.

[12] J. Lindhard, M. Scharff, and H. E. Schiøtt, Mat. Fys. Medd. Dan. Vid. Selsk. 33 (1963) No. 14.

[13] W. Schilling, K. Schroeder, and H. Wollenberger, Phys. Stat. Solidi 38 (1970) 245.

[14] P. Jung, R. L. Chaplin, H. J. Fenzl, K. Reichlet, and P. Wombaugh, Phys. Rev. B 8 (1973) 553.

[15] O. S. Oen, Oak Ridge National Laboratory Report ORNL-4897 (1973).

[16] M. T. Robinson, Proc. Intern. Conf. Radiation-Induced Voids in Metals, (Albany, NY, 1971) p. 397.

[17] D. G. Doran, R. L. Simons, and W. M. McElroy, Properties of Reactor Structural Alloys After Neutron or Particle Irradiation (ASTM, Philadelphia, 1975) p. 290.

[18] K. L. Merkle, Phys. Stat. Solidi 18 (1966) 173.

[19] R. S. Averback, R. Benedek and K. L. Merkle, J. Nucl. Mater. 75 (1978) 162 and Phys. Rev. B, in press.

[20] M. A. Kirk and L. R. Greenwood, to be published.

[21] J. B. Roberto, C. E. Klabunde, J. M. Williams, and R. R. coltman, Jr., J. Nucl. Mater. 73 (1978) 97.